Predicting Shear Transformation Events in Metallic Glasses

Bin Xu, Michael L. Falk, J. F. Li, and L. T. Kong

Phys. Rev. Lett. **120**, 125503 — Published 22 March 2018

DOI: 10.1103/PhysRevLett.120.125503

Predicting shear transformation events in metallic glasses

Bin Xu,[1] Michael L. Falk,[2,*] J. F. Li,[1] and L. T. Kong[1,†]

[1] *State key Laboratory of Metal Matrix Composites, School of Materials Science & Engineering, Shanghai Jiao Tong University, Shanghai 200240, China*

[2] *Department of Materials Science and Engineering, Mechanical Engineering, and Physics and Astronomy, Johns Hopkins University, Baltimore, Maryland 21218, USA*

(Dated: February 20, 2018)

Abstract

Shear transformation is the elementary process for plastic deformation of metallic glasses, the prediction of the occurrence of the shear transformation events is therefore of vital importance to understand the mechanical behavior of metallic glasses. In this letter, from the view of potential energy landscape, we found that the protocol-dependent behavior of shear transformation is governed by the stress gradient along its minimum energy path and we propose a framework as well as an atomistic approach to predict the triggering strains, locations, and structure transformations of the shear transformation events under different shear protocols in metallic glasses. Verification with a model $Cu_{64}Zr_{36}$ metallic glass reveals that the prediction agrees well with athermal quasi-static shear simulations. The proposed framework is believed to provide an important tool for developing a quantitative understanding of the deformation processes that control mechanical behavior of metallic glasses.

* mfalk@jhu.edu

† konglt@sjtu.edu.cn

The lack of long range order in metallic glasses (MGs) imparts them with unique mechanical properties [1–5]. It also imposes great challenges in understanding their mechanical behavior, since models based on dislocations, which control the plastic deformation in crystalline materials, are not applicable. Substantial efforts have been devoted to develop new models [6–12] that can account for the mechanical behavior of MGs. One common feature of many such models is that the local rearrangement of small numbers of atoms, referred to as a shear transformation (ST), is generally accepted as the elementary process for plastic deformation in MGs. A thorough understanding of the ST events is believed to be the key to elucidate the plastic response and failure modes of MGs. In this regard, it has been argued that ST events correlate with "regions of high free volume", "soft spots", or "lowest frequency normal mode" [12–17]. Nonetheless, it was found that the triggering of ST events is rather protocol-sensitive [18], suggesting that the structural information examined by previous models is insufficient to draw a full picture of the activation of the ST events. In this letter, we will show that information on the stress gradient of the energy landscape is of vital importance to understand the protocol-sensitive behavior of the ST events. And by exploring the energy landscape, we propose a theoretical framework to predict the occurrence of ST events under different shear protocols, including their triggering strains, locations and structure transformations.

Following the analytical framework proposed by Maloney et al. [12], under athermal quasi-static shear, the motion of an amorphous system can be expressed as

$$\frac{d\boldsymbol{r}}{d\gamma} = -\boldsymbol{H}^{-1} \cdot \boldsymbol{\Xi}, \tag{1}$$

where $\boldsymbol{r} = \{r_i(\gamma)\}$ are the atomic positions of the system in a reference cell [12], γ is the macroscopic shear strain, $\boldsymbol{H} = (\partial^2 U/\partial r_i \partial r_j)$ is the Hessian matrix, $U = U(\boldsymbol{r}, \gamma)$ is the potential energy, and $\boldsymbol{\Xi} = (\partial^2 U/\partial r_i \partial \gamma)$. Eq. 1 can be further decomposed into the directions along the eigenvectors of the Hessian matrix as [12]

$$\frac{d\boldsymbol{r}}{d\gamma} = -\sum_p \frac{\xi_p}{\lambda_p} \boldsymbol{\Psi}_p, \tag{2}$$

where $\boldsymbol{\Psi}_p$ is the eigen vector of the Hessian matrix, λ_p is the eigen value, and ξ_p is the decomposition factor of $\boldsymbol{\Xi}$: $\boldsymbol{\Xi} = \sum_p \xi_p \boldsymbol{\Psi}_p$. Eq. 2 shows that the weight factor ξ_p/λ_p flags the mode that dominates the motion of the system. That is, modes with a large ξ_p/λ_p ratio will dominate the motion of the system. It has been argued that low frequency modes with small

values of λ_p correspond to the dominating ones [12, 16]. However, we will show later that ξ_p is the key to understand and to predict the protocol-dependent behavior of the triggering of the ST events, since it incorporates the protocol information, and therefore ξ_p/λ_p rather than λ_p is the quantity of concern. For simplicity, let us first consider a scenario where only one dominating mode exists, the multi-dimensional problem can be simplified into a one-dimensional one. Assuming that the dominating mode Ψ^* remains unchanged under different macroscopic shear strain levels (γ), the motion of the system can be represented by the variation of the reaction coordinate x which satisfies $\boldsymbol{r} - \boldsymbol{r_0} \approx x\boldsymbol{\Psi^*}$, where $\boldsymbol{r_0}$ represents the initial configuration at the reference macroscopic shear strain γ_0. The equation of motion Eq. 2 can be rewritten as

$$\frac{\mathrm{d}x}{\mathrm{d}\gamma} = -\frac{\xi^*}{\lambda^*} = -\frac{\partial}{\partial x}\left(\frac{\partial U}{\partial \gamma}\right)\left(\frac{\partial^2 U}{\partial x^2}\right)^{-1} = -V\frac{\partial \tau}{\partial x}\left(\frac{\partial^2 U}{\partial x^2}\right)^{-1}, \tag{3}$$

where $\frac{\partial U}{\partial \gamma} = V\tau$ is used in the deduction. Clearly, in the one-dimensional case, $\xi^* = V\frac{\partial \tau}{\partial x}$. As has been demonstrated in our previous work [19], Eq. 3 can be solved by numerical integration if the whole one-dimensional energy landscape is known. Supposing there exists a first order saddle point for the associated ST event at the reference strain level locating at $x_s(\gamma_0) = x_s^0$, with an energy barrier of $Q(\gamma_0) = Q_0$. If the corresponding minimum energy path (MEP) can be approximated by a cubic polynomial (which has often observed in MGs as a fold catastrophe [12, 20]), and the stress gradient $\frac{\partial \tau}{\partial x}$ remains constant for any x, then the solution of the above equation of motion can be expressed analytically, and information on the initial minimum and the transition state configuration at the referential strain level will be sufficient to define the unknown parameters [19]. Especially, the critical macroscopic shear strain at which the ST event will be triggered would be given by [19]:

$$\begin{aligned} \gamma_c - \gamma_0 &= -\frac{3Q_0}{2V\Delta\tau_0} = -\frac{\lambda^* x_s^0}{4V\xi^*}, \\ \Delta\tau_0 &= \frac{\partial \tau}{\partial x}x_s^0 = \tau(x_s^0, \gamma_0) - \tau(0, \gamma_0). \end{aligned} \tag{4}$$

Although the above deduction is based on a scenario with only one dominating mode, it can be easily proven that the solution of Eq. 5 is also valid in case multiple dominating modes exist in the system, only if they are independent from each other. This requirement will be satisfied when the ST events are sparse and localized in space. Eq. 5 suggests that the mode with a small eigen value λ^* while a large stress gradient (hence a large ξ^*) — in turn a large ξ^*/λ^* ratio — will reach the critical/triggering macroscopic shear strain γ_c first.

In other words, the ST events in an athermal quasi-static shear process correlate with modes with a large ξ/λ ratio. To clearly reveal the quantity that governs the protocol-dependent behavior of STs, Eq. 5 is rewritten as

$$\gamma_{c,\alpha\beta} - \gamma_{0,\alpha\beta} = -\frac{3Q_0}{2V\Delta\tau_{0,\alpha\beta}} = -\frac{3Q_0 x_s^0}{2V}\left(\frac{\partial\tau_{\alpha\beta}}{\partial x}\right)^{-1}, \tag{5}$$

by incorporating the shear protocol explicitly, where α, β enumerates x, y, or z ($\alpha \neq \beta$). One sees clearly that the protocol dependence of the ST event originates from the stress gradient $\frac{\partial\tau_{\alpha\beta}}{\partial x}$ of the corresponding mode (or MEP), since Q, V and x_s^0 are apparently protocol independent. Depending on the orientation of the macroscopic shearing imposed, the variation of the shear stress can be either uphill or downhill, i.e., the shear stress gradient can be either negative or positive. Its sign determines whether the ST event can be triggered in the current athermal shear direction or not, while its magnitude together with other terms in Eq. 5 determines the triggering strain of the ST event. In the supplemental material, the stress variation along the MEP of a typical ST event is shown for reference. Whereas, by exploring the energy landscape of the MG or at least locating the first order saddle points corresponding to all possible ST events, Eq. 5 enables one to predict the triggering point of each event when the MG is subject to shear.

To this end, several methods have been developed during the past years to search for the first order saddle points of a given system, among them the activation-relaxation technique nouveau (ARTn) [21–23] is the most widely used one in exploring the energy landscape of metallic glasses [24–28] as prior knowledge of the final state is not required. In this letter, ARTn will be employed to harvest the ST events in a $Cu_{64}Zr_{36}$ MG model, which contains 10000 atoms in total and was generated with a cooling rate of 10^9 K/s. This model was also used in our previous work [19]. The "activation" was initiated by imposing a random displacement to the local cluster centered on a chosen atom with a radius of 3.7 Å, which corresponds to the first minimum of the pair correlation function of the $Cu_{64}Zr_{36}$ MG. During the "relaxation" process, a force tolerance of 5×10^{-3} eV/Å was used for converging to the saddle points and a relatively strict tolerance of 1×10^{-4} eV/Å was adopted for the local minima. In principle, to predict all the ST events that will be triggered during the deformation process, one needs to identify all the unique events in the system. **While in practice, a reasonable prediction can be made by sampling a relatively limited number of first order saddle points harvested. One possible reason is the bias of**

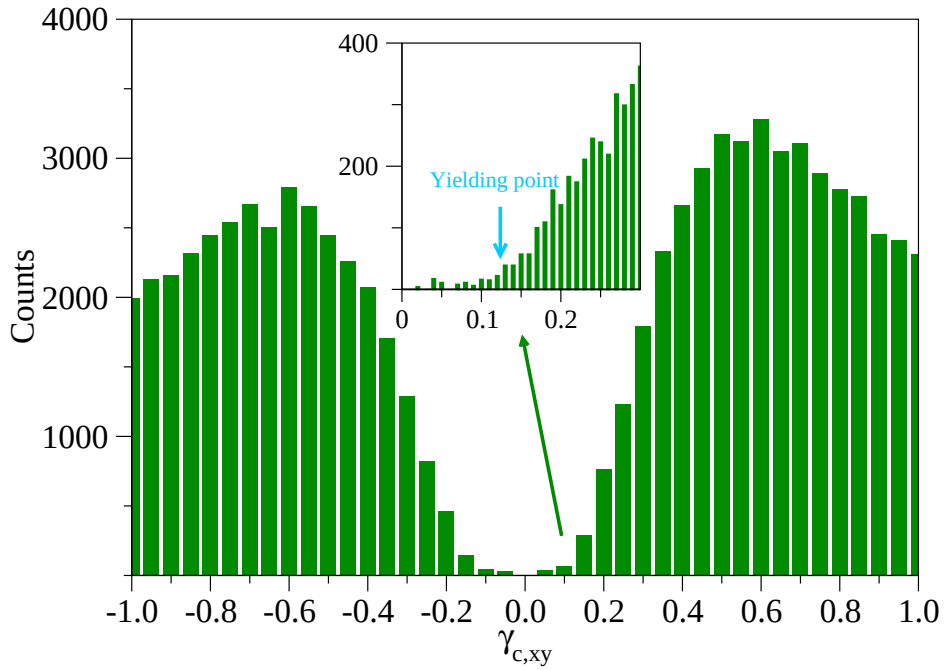

FIG. 1. The distribution of triggering strains (between −100.00% and 100.00%) for xy shear of all the events harvested. The inset highlights the distribution of triggering strain between 0.00% and 30.00%.

ARTn method towards low barriers [29], but this problem has not been discussed extensively in the literature and further work is needed to confirm the ability of ARTn to sample low energy barriers comprehensively. Inasmuch, multiple activations were attempted for each cluster until 20 events were found and 200, 000 events in total were therefore harvested for the unstressed glass model. With the information obtained from the ARTn calculations, the triggering strains for each event under different loading conditions was then estimated following Eq. 5.

Fig. 1 shows the distribution of the deduced triggering strains for the ST events harvested upon xy shearing. It is seen that under small strains, only relatively few ST events can be triggered, while at large strains large number of events can be triggered. Nevertheless, for events with large predicted triggering strains, many of the events are correlated rather than independent from each other. As a result, the applicability of the present approach at this regime is in question. We will therefore focus on the events with small triggering strains which are independent to each other (triggered in different regions). There are 18 events with triggering strains in the range of $0.00\% < \gamma_{xy} < 5.00\%$, and only four of

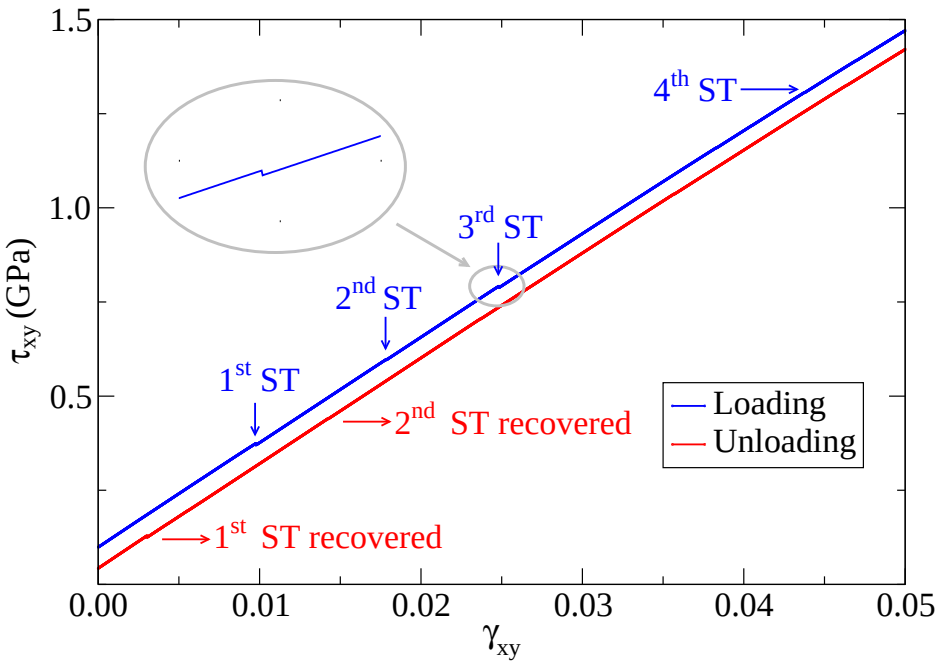

FIG. 2. Loading (blue line, from shear strain 0.00% to 5.00%) and unloading (red line, from shear strain 5.00% to 0.00%) stress-strain curves for xy shearing. The loading curve is shifted upwards by +0.005 GPa for clarity. Four shear transformation events were found corresponding to the stress drops on the loading curve. The first two events was recovered during the subsequent unloading deformation.

them are found to be distinct by comparing their transition state and minimum-energy configurations: the same event can be searched multiple times by ARTn when initiated by different perturbations. The full MEP of these four events are then calculated by using the nudged elastic band (NEB) method. Based on the information from the NEB calculations the respective triggering strains of these events are re-predicted (refined) by using the full numerical integration [19] instead of the analytical approximation of Eq. 5. Two more events are ruled out according to the re-prediction (The appendix in Ref. [19] illustrated a typical example that should be ruled out). Thus, only two events are predicted to be triggered with critical shear strains in the range of $0.00\% < \gamma_{xy} < 5.00\%$.

Similar analysis are also performed for xz and yz shearings, and in total 7 distinct events that can be triggered within a macroscopic strain of $|\gamma_{\alpha,\beta}| = 5.00\%$ are identified upon all 6 simple shearings.

To confirm the predicted triggering of these events, athermal quasi-static shear (AQS)

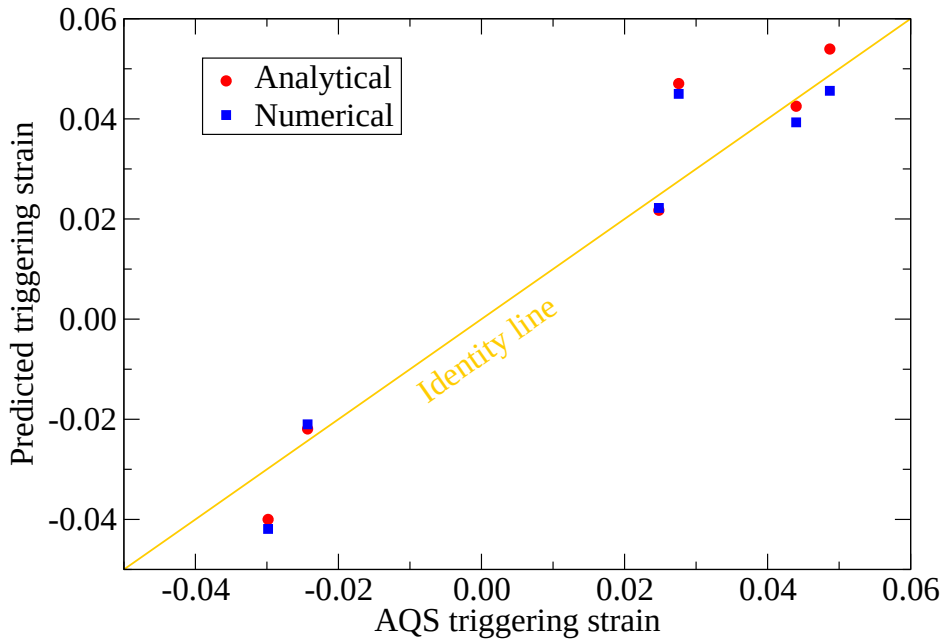

FIG. 3. The analytically predicted triggering strains (red circles, following Eq. (5)) and the numerically predicted triggering strains (blue squares, following the full numerical integration [19] versus the AQS values).

simulations [12] with simple xy, $-xy$, xz, $-xz$, yz and $-yz$ shearings are performed at a step size of 1×10^{-5}. Fig. 2 shows the stress-strain curve for the xy shearing, where four sudden drops of the stress are identified from the loading curve for $\gamma_{xy} \leq 5.00\%$. Each drop should correspond to an ST event. By comparing the triggering strains of these events to the predicted ones, one finds that the 3$^{\text{rd}}$ and the 4$^{\text{th}}$ AQS events match well with the two predicted ones upon xy shearing. Further analysis reveals that each of the 7 predicted distinct events can be matched with a triggered AQS event, and Fig. 3 compares the predicted triggering strains with their respective AQS counterpart. One sees that the agreement is reasonably good, with a root mean square error of 0.80% between the triggering strains from AQS and the prediction.

The ARTn method also reveals the structure transformations of each event, which can be compared with AQS simulations. To achieve this, the von-Mises atomic shear strains [30] are evaluated by taking the initial undeformed configuration as the reference. Fig. 4 shows the shear transformed atoms for each independent event, by selecting those atoms with a atomic von-Mises strain greater than 0.01 as "shear transformed atoms". One sees from Fig. 4 that the shapes and locations of the local clusters associated with these events predicted based on

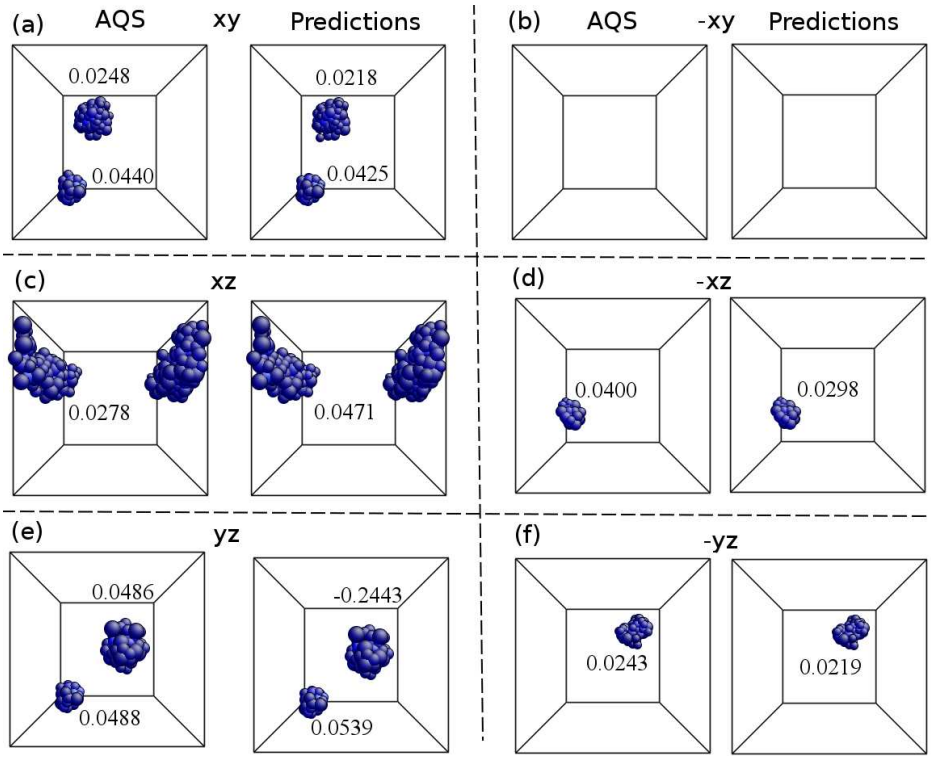

FIG. 4. Comparison of the local configurations of the ST events between the predictions and AQS simulations. Atoms were colored according to their respective atomic von-Mises strain [30] taking the initial undeformed configuration as a reference, and only those with an atomic von-Mises strain greater than 0.01 are shown. For each case, the left one is identified by AQS loading and unloading, and the right one is predicted based on ARTn. The triggering strains calculated from Eq. (5) and simulated from AQS are annotated around local cluster. All the predicted triggering strains are close to simulation results, except for the right one in (e). The possible reason is discussed in the text.

ARTn calculations agree well with those from AQS simulations, suggesting that the current model is indeed capable of predicting the occurrence of the ST events and the locations of STZs with reasonable accuracy. The predicted structure transformations of those ST events were also further confirmed by comparing the displacement field of those "shear transformed atoms", and the relative errors (defined in supplemental materials) are within 2%.

Nevertheless, we are also curious about the first two events observed in Fig. 2. Why are they not predicted by the current model? To reveal the reason behind this, AQS unloading simulations were also performed. A careful inspection of the unloading curve shown in Fig. 2

finds that the first two events are recovered during the unloading process, while the other two are not: a "negative" (reversed) loading is needed for the latter two to be recovered. This suggests that in MGs, at least two kinds of shear transformations can be triggered: one of them can be seen as a local "anelastic" transformation [8], as there is local atomic rearrangement that can be recovered upon unloading. The other one is a "viscoplastic" transformation [8] that cannot recover spontaneously upon unloading. The first order saddle saddle point of an ST event exists only when the macroscopic shear strain lies in between the triggering and the recovering strains of the event. For the "anelastic" events, the associated local clusters are unstable in the undeformed state, and consequently no "transition state" can be found, no matter what sampling/searching technique is employed. The events harvested here correspond to the latter case only, which have well-defined equilibrium and transition states.

One may notice that the current approach made a rather poor prediction on the triggering strain for one of the events. As is seen in Fig. 4(e), the AQS event that occurs at $\gamma_{xz} = 4.86\%$ is predicted to have a triggering strain of -24.43%. Detailed analysis of the deformation process associated with this event reveals a neighboring cluster that undergoes "anelastic" event at a macroscopic strain of $\gamma_{xz} = 2.35\%$, which means that these two events are correlated with each other, violating the basic assumption that the ST events are independent from each other. To confirm this, we re-sampled the energy landscape of the local region associated with this event, taking a macroscopic strain of $\gamma_{xz} = 4.00\%$ as the referential state, where the interfering event has been triggered. The predictions made based on the newly sampled MEP gives a triggering strain of 4.98%, which is now close to the AQS result of 4.86%. Excluding this case, we would like to emphasize that nearly all the "viscoplastic" transformations were successfully predicted as seen in Fig. 4. **To further demonstrates the validity/reliability of the current approach, three other MG samples were also tested. The details of samples can be found in the supplemental material; the correlation between the AQS triggering strains and the predicted ones in all the four samples is shown in Fig. 5. It is seen that the present model works very well for events with small strains ($< 2\%$), while the scatter increases substantially for large strains where high-order nonlinear effect becomes important.**

In summary, the protocol-dependent behavior of ST events is found to be governed by the

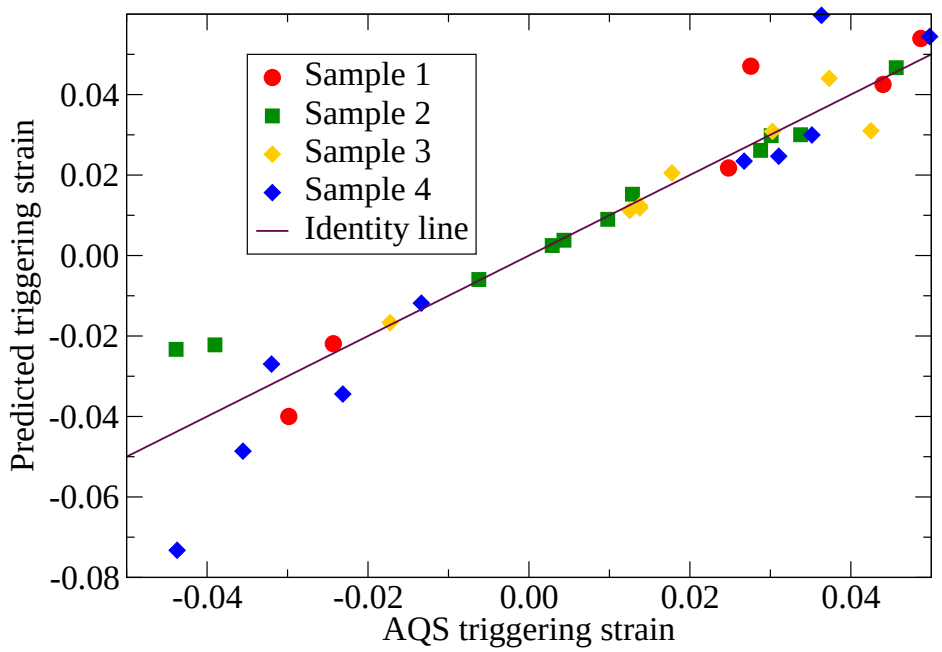

FIG. 5. The AQS triggering strains versus the predicted ones (following Eq. (5)) for all predicted events in the four samples investigated.

stress gradient along the MEP of the events, and a framework to locate and characterize the occurrence of ST events in metallic glasses is proposed. Verification based on atomistic simulations reveals that by effectively capturing the features of the PEL associated with the shear transformation events, the predicted triggering strains, locations and structure transformations agree well with that from athermal quasi-static shearing simulations. Nonetheless, the "anelastic" events that would recover upon unloading were not captured. Exploring the PEL is known to be an indispensable way to understand the complex phenomenology in metallic glasses [31–33]. The thermal activation events in the PEL has been discussed and used to understand the structure and energy evolution based on thermal histories [28]. In terms of the mechanical activation of those events, the presently proposed framework as well as the verification demonstrated suggests that it is possible to model and predict the mechanical behavior of metallic glasses by examining the PEL, which therefore provides an important tool to uncover the secrets underlying the structural state and, thereby, the mechanical behavior of metallic glasses.

B.X. and L.T.K. acknowledge financial support by the National Key R&D Program of China (2017YFB0701501), the National Natural Science Foundation of China (NSFC,

Grants No. 51620105012 & 51271114), and MaGIC of Shanghai Jiao Tong University. M.L.F. acknowledges support provided by NSF Grant Awards No. 1408685/1409560. Computing facility from the π cluster at Shanghai Jiao Tong University is also acknowledged.

---

[1] C. A. Schuh, T. C. Hufnagel, and U. Ramamurty, Acta Mater. **55**, 4067 (2007).

[2] Y. Q. Cheng and E. Ma, Prog. Mater Sci. **56**, 379 (2011).

[3] M. L. Falk and J. Langer, Annu. Rev. Condens. Matter Phys. **2**, 353 (2011).

[4] S. Takeuchi and K. Edagawa, Prog. Mater Sci. **56**, 785 (2011).

[5] W. H. Wang, Prog. Mater Sci. **57**, 487 (2012).

[6] F. Spaepen, Acta Metall. **25**, 407 (1977).

[7] A. Argon, Acta Metall. **27**, 47 (1979).

[8] A. Argon and L. Shi, Acta Metall. **31**, 499 (1983).

[9] V. V. Bulatov and A. S. Argon, Modell. Simul. Mater. Sci. Eng. **2**, 167 (1994).

[10] M. L. Falk and J. S. Langer, Phys. Rev. E **57**, 7192 (1998).

[11] W. L. Johnson and K. Samwer, Phys. Rev. Lett. **95**, 195501 (2005).

[12] C. Maloney and A. Lemaître, Phys. Rev. Lett. **93**, 195501 (2004).

[13] T. C. Hufnagel, C. A. Schuh, and M. L. Falk, Acta Mater. **109**, 375 (2016).

[14] M. Mosayebi, P. Ilg, A. Widmer-Cooper, and E. Del Gado, Phys. Rev. Lett. **112**, 105503 (2014).

[15] S. Patinet, D. Vandembroucq, and M. L. Falk, Phys. Rev. Lett. **117**, 045501 (2016).

[16] J. Ding, S. Patinet, M. L. Falk, Y. Cheng, and E. Ma, Proc. Natl. Acad. Sci. U.S.A. **111**, 14052 (2014).

[17] F. Boioli, T. Albaret, and D. Rodney, Phys. Rev. E **95**, 033005 (2017).

[18] O. Gendelman, P. K. Jaiswal, I. Procaccia, B. Sen Gupta, and J. Zylberg, Europhys. Lett. **109**, 16002 (2015).

[19] B. Xu, M. Falk, J. Li, and L. Kong, Phys. Rev. B **95**, 144201 (2017).

[20] D. J. Wales, Science **293**, 2067 (2001).

[21] N. Mousseau and G. T. Barkema, Phys. Rev. E **57**, 2419 (1998).

[22] E. Cancès, F. Legoll, M.-C. Marinica, K. Minoukadeh, and F. Willaime, The J. Chem. Phys. **130**, 114711 (2009).

[23] N. Mousseau, L. K. Béland, P. Brommer, J.-F. Joly, F. El-Mellouhi, E. Machado-Charry, M.-C. Marinica, and P. Pochet, J. At., Mol., Opt. Phys. **2012**, 1 (2012).

[24] D. Rodney and C. Schuh, Phys. Rev. Lett. **102**, 235503 (2009).

[25] Y. Fan, T. Iwashita, and T. Egami, Nat. Commun. **5**, 5083 (2014).

[26] Y. Fan, T. Iwashita, and T. Egami, Phys. Rev. Lett. **115**, 045501 (2015).

[27] F. Delogu, Scr. Mater. **113**, 145 (2016).

[28] Y. Fan, T. Iwashita, and T. Egami, Nat. Commun. **8**, 15417 (2017).

[29] F. Valiquette and N. Mousseau, Phys. Rev. B **68**, 125209 (2003).

[30] F. Shimizu, S. Ogata, and J. Li, Mater. Trans. **48**, 2923 (2007).

[31] P. G. Debenedetti and F. H. Stillinger, Nature **410**, 259 (2001).

[32] D. J. Lacks and M. J. Osborne, Phys. Rev. Lett. **93**, 255501 (2004).

[33] F. H. Stillinger, Science **267**, 1935 (1995).